International Journal of Mechanical and Production Engineering Research and Development (IJMPERD)
ISSN(P): 2249-6890; ISSN(E): 2249-8001
Vol. 8, Issue 3, Jun 2018, 1067-1084

Original Article

INFLUENCE OF FUNCTIONALIZED MULTI-WALLED CARBON NANOTUBES ON THE MECHANICAL PROPERTIES AND DELAMINATION IN DRILLING OF CFRP COMPOSITES

SWAPNIL SUMAN, P PANCHAM ALVA, NOEL GEORGE DANIEL & NAGARAJA SHETTY

Department of Mechanical and Manufacturing Engineering, Manipal Institute of Technology, MAHE, Manipal, India

ABSTRACT

A study was conducted on the influence of adding carboxyl functionalized multi-walled carbon nano tubes (COOH-MWCNTs) as a filler to carbon fibre reinforced plastics (CFRP) on tensile and flexural properties. In addition to it, the effects of COOH-MWCNTs on delamination of drilled holes in CFRP laminates were also examined. Tensile and flexural tests were performed on a universal testing machine according to ASTM standards. The tensile strength and Young's modulus of MWCNTs modified CFRP nano composites increased by31.4% and 18% respectively compared to neat CFRP while the enhancements in flexural strength and flexural modulus were 43% and 35.2% respectively. Drilling tests were conducted on CFRP laminates fabricated with neat and MWCNTs filled epoxy matrix. The drilling process parameters evaluated were feed rate, spindle speed, drill diameter and point angle of the drill bit. The delamination analysis of CFRP laminate was performed using digital image processing and adjusted delamination factor was used as a measure of delamination. Using response surface methodology (RSM), the effects of cutting parameters on delamination were analysed. The delamination was observed to decrease with an increase in spindle speed while an increase in feed rate, point angle and drill diameter led to an increase in delamination. The addition of nanotubes to the CFRP composite resulted in an average reduction of adjusted delamination factor by 25.74%.

KEYWORDS: Delamination, Multi-Walled Carbon Nanotubes, Response Surface Methodology, CFRP, Tensile & Flexural Properties

Received: Apr 23, 2018; **Accepted:** May 14, 2018; **Published:** Jun 19, 2018; **Paper Id.:** IJMPERDJUN2018112

INTRODUCTION

In the last few years the demand for CFRP composites has increased considerably, due to their widespread application in aerospace, automotive and marine industries [1]. One of the crucial operations in machining CFRP composites is drilling [2]. Drilling is performed to make holes in the CFRP for fastening and part assembly [3,4]. The abrasive nature, anisotropy and non-homogeneity of CFRP composites causes different kinds of damages during drilling. Some of the most common problems that occur during drilling of CFRP composites are fibre pull-out, fibre–matrix de-bonding, micro cracking and delamination at the entry and exit layers [5]. Most prominent damage observed was of delamination [6]. Delamination leads to poor assembly tolerance, reduction in structural integrity and can cause deterioration in the long run [7]. In the aircraft industry, 60% of the

parts made of composite laminates were excluded because of drilling induced delamination [2].

Peel up and push out are the most common modes of delamination reported [8,9]. Peel up delamination happens when cutting edge of drill bit makes contact with the composite, the force acts through the slope of the drill bit flute resulting in separation of the laminates from one another. Push out delamination happens at the exit when the uncut ply below the drill bit becomes more vulnerable to deformation due to reduction in its thickness. Peel-up delamination is less than push-out delamination [10]. The push-out delamination can be reduced by using a support plate under the work piece [11]. It was also found that the critical thrust force increases by using a backup plate which allows drilling at high feed rates before delamination occurs [12]. Murphy et al. conducted an experiment to study the effects of thrust force and torque during drilling of CFRP and found the generation of maximum thrust force took place when the last ply of the laminates was pushed by the drill bit. On the other hand the maximum torque was found at the entrance of the laminate [13]. One of the key parametersduring drilling to describe machinability of CFRP laminates is thrust force because it directly affects the quality of drilled holes and thereby delamination factor [14]. Thrust force and delamination factor have a direct relationship, thus drilling-induced delamination can be minimised by reducing the thrust force [15]. Heisel et al. [16] found that that the point angle has substantial effect on delamination factor. Drill bit materials also have a significant role in delamination reduction [17,18]. Feito et al. [19] observed that the thrust force and torque increased with feed rate while they decreased with an increase in spindle speed.

Karimi et al. studied the effect of MWCNTs on drilling induced delamination. They found that the main parameters that affected delamination were nano content, feed rate and spindle speed. Drill diameter was found to have the least effect. It was seen that delamination increases with increasing feed rate and decreasing cutting speed. Nano content decreased delamination in the beginning but it started increasing at 0.5 wt.%. Using interaction plots it was seen that the drill diameter showed high interaction with cutting speed and feed rate. Cutting speed and feed rate also had high interaction [20]. Kumar et al. found that functionalization of nanotubes (CNT) increased their dispersion in solvent and also improved the adhesion between matrix and CNTs due to dipole-dipole and hydrogen bonding forces that act between nanotubes and matrix. The microscopic study of the hole walls showed that, there is reduction in fibre fracture, debonding, and matrix pull-out with increase in MWCNTs. They found maximum delamination in the case of neat CFRP composite materials and proposed that it could have been due to failure of inter-laminar bond between plies [21]. Improper dispersion of carbon nanotubes reduces its capability as reinforcement and the carbon nanotubes slip over each other when force is applied to the composite [22]. The most common methods to disperse the carbon nanotubes are ultra sonication, high shear mixing, use of surfactants, surface functionalization or a combination of the above methods [23, 24]. For application involving load bearing, functionalizing with covalent groups is most effective since the covalent bonds at the interface allow for improved transfer of load [25]. Good dispersion of MWCNTs in epoxy mixture results in increased viscosity therefore breather and release film have to be applied to MWCNT resin mixture while performing hand layup [26].

Use of carbon nano tubes as filler material in CFRP has been shown to improve flexural strength, tensile strength, inter laminar shear strength which have important application in aircraft design [27]. Li et al. [26] found that MWCNTs modified CFRP composites result in higher mode I inter laminar fracture toughness than neat CFRP composites. Gojny et al. [28] found through transmission electron microscope (TEM) study that there is an increase in interfacial interaction between the functionalized nanotubes and matrix. Abdelal et al. [29] found that when CNTs were infused onto the carbon fibre surface, the tensile strength of the carbon fibre increased by more than 14%. Gojny et al. found that functionalised

nanotubes composite had higher value of Young's Modulus compared to non-functionalised nano tubes composite. They attributed this to the improved dispersibility in the polar epoxy resin because of better interactions with the polar amino-groups [30]. Telescopic pull out is the most common type of mechanism of failure for MWCNTs under tensile load. The outermost layer remains strongly bonded to the matrix whereas cracking takes place in the inner tube bridges. The inner shells are bonded by Van der Waals force which is weak compared to covalent bond [28]. Jahan et al. [31] found that the tensile strength and Young's Modulus was 50% and 35% better in COOH-MWCNT over neat composites and this was mainly attributed to improved interfacial interaction and dispersion between the epoxy matrix and MWCNTs.

Islam et al. [32] conducted 3 point bending test and found that addition of MWCNTs led to an increase in flexural strength and modulus of all the samples. Zhou et al. [33] found that the flexural strength and modulus in small loadings were improved because of the dispersion of CNTs which restricted the movement of the polymer chains. They added that the modulus of nano phased epoxy increased continuously with higher CNT content when the range of MWCNT content was 0.1%-0.4%by weight. Although the addition of 0.4 wt% of MWCNTs caused an improvement in flexural modulus, the strength decreased. Hence, they concluded that0.3% wt. MWCNTs loading resulted in highest improvement in flexural strength as compared with 0.1, 0.2 and 0.4% wt. of CNT.

MATERIALS AND METHODS

Tensile and Flexural Test Specimen Preparation

The materials used for the specimen preparation were 200 GSM Bi-directional carbon fibre obtained from Arrow Technical Textiles Pvt. Ltd., Mumbai, India and epoxy resin LY556 along with hardener HY951 obtained from Singhal Chemical Corporation, Uttar Pradesh, India. Bidirectional carbon fibre was used because it has maximum strength and stiffness along all directions [1]. The MWCNTs used had been surface functionalised using carboxyl groups (-COOH) obtained from Platonic Nanotech Private Limited, Jharkhand, India. Their degree of functionalisation was 10% and they had a diameter in the range of 12-15 nm and length ranging from 3-10 microns. Their specific surface area (SSA) was in the range of 250-270 m^2/g. The MWCNTs had a purity >97%. Two sets of specimens, neat CFRP and CFRP doped with MWCNTs were prepared. 0.3% wt. MWCNTs were added to the epoxy, and an ultra sonicator {Grant XUBA 3 Ultrasonic water bath} was used for half an hour to disperse the MWCNTs uniformly in the epoxy. The mixture of epoxy and hardener was in 10:1 ratio. The fabrication of laminates was done by hand lay-up process, keeping the carbon fibre at 55% by weight and resin content at 45% by weight and was placed in a vacuum bagging setup for 24 hours at room temperature. The specimen was post cured in a hot-air oven at temperatures 50°C, 70°C and 85°C in time intervals of 30, 60 and 120 minutes respectively. For tensile testing the specimens were cut using a circular saw into the dimensions of 200mm x 25mm x 2mm according to ASTM 3039-17. Emery cloth was fixed at the ends of the tensile specimen which acts as a gripping surface. For flexural test, specimens were cut using a circular saw into the dimension of 100mm x 12.7mm x 3mm according to ASTM D790-17. Three samples for each test were prepared.

Fabrication of Composite for Drilling Tests

Two composite plates of dimensions 200mm x 200mm x 5mm were fabricated using the above methods for performing drilling tests to analyse the delamination of drilled holes. Composites with neat epoxy and 0.3% wt. COOH-MWCNTs filled epoxy were fabricated.

Design of Experiments using Response Surface Methodology (RSM)

RSM is used to design the layout of experiments. It is a statistical technique based on multiple regressions to help in the design, analysis and optimisation of the responses. Central composite design (CCD) is used here since it needs the lowest number of experiments to find the relationship between the response and the parameters without loss of accuracy [34]. RSM design needs minimum three levels for each factor. The response in drilling of composite in CFRP is represented by "Y" which is called the response surface given by:

$$Y = f(A, B, C, D) \quad (1)$$

The second order model developed by quadratic regression analysis is used which has an approximation function given by:

$$Y = \gamma_0 + \gamma_1 A + \gamma_2 B + \gamma_3 C + \gamma_4 D + \gamma_{11} A^2 + \gamma_{22} B^2 + \gamma_{33} C^2 + \gamma_{44} D^2 + \gamma_{12} AB + \gamma_{13} AC + \gamma_{14} AD + \gamma_{23} BC + \gamma_{24} BD + \gamma_{34} CD \quad (2)$$

where, γ_0 is the constant term, γ_i are the linear terms, γ_{ii} are the square terms and γ_{ij} represents the interaction between the factors. The factors spindle speed, feed rate, drill diameter and point angle were examined at three levels and are presented in Table 1. MINITAB 14.0 software was utilised for designing the experiment, obtaining coefficients of equation (2) and response optimising. The design here constituted of 30 experiments with the following combinations of the four drilling parameters as shown in Table 2.

Table 1: Process Parameters and their Levels

Symbol	Parameters	Level 1	Level 2	Level 3
A	Spindle Speed (rpm)	1200	1500	1800
B	Feed Rate (mm/min)	10	15	20
C	Point Angle (degree)	90	104	118
D	Drill Diameter (mm)	4	6	8

Table 2: Experimental Design Layout using RSM

Spindle Speed(rpm)	Feed Rate(mm/min)	Point Angle(degree)	Drill Diameter(mm)
1200	10	90	4
1800	10	90	4
1200	20	90	4
1800	20	90	4
1200	10	118	4
1800	10	118	4
1200	20	118	4
1800	20	118	4
1200	10	90	8
1800	10	90	8
1200	20	90	8
1800	20	90	8
1200	10	118	8
1800	10	118	8
1200	20	118	8
1800	20	118	8
1500	15	104	6
1500	15	104	6
1500	15	104	6
1500	15	104	6
1200	15	104	6

Table 2: Contd.,			
1800	15	104	6
1500	10	104	6
1500	20	104	6
1500	15	90	6
1500	15	118	6
1500	15	104	4
1500	15	104	8
1500	15	104	6
1500	15	104	6

Experimental Procedure

Tensile and Flexural tests

The tensile test specimens were tested using auniversal testing machine {UNITEK 9450} with a maximum load of 50kN. The crosshead speed was set to 2mm/min. The tensile strength, Young's modulus and the stress-strain graphs were obtained. The failure mode was characterised based on the damage and location according to ASTM 3039-17.

Three point bending tests were performed on the flexural specimens prepared according to ASTM D790-17. It was performed using a universal testing machine {UNITEK 9450} which has a maximum load of 50kN. The crosshead speed was set to 5.5 mm/min. The flexural strength at failure was calculated.

Drilling tests on CFRP composites with and without MWCNTs

Titanium nitride (TiN) coated solid carbide twist drill bit with different drill diameters and point angles as shown in Figure 1 were used in this experiment. The drilling operation was conducted using computer numerical control (CNC) machine {AMC DTC 300 vertical machining centre}. The application of support plates allowed a reductionin push-down delamination[11].

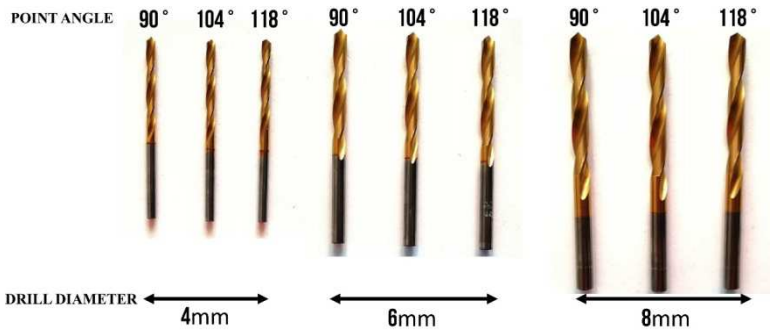

Figure 1: Specifications of Twist Drill Bits used

Measurement of Delamination

Measurement of delamination is only of surface level delamination where the damaged area is externally exposed and visible; internal delamination is not considered. Delamination at the exit side of the hole (push out delamination) was measured. The images of the drilled holes were obtained using a high resolution scanner {Epson GT 20000, 9600 dpi}. Image J 1.52b software was used to process the scanned image. The image was converted to an 8-bit binary image. A threshold filter was used to remove the unwanted points in the image and make the image suitable for measuring the delamination factor. This process is shown in Figure 2.

Delamination factor (F_d) [35] is defined as the ratio of the maximum diameter of delamination (D_{max}) to the diameter of drilled hole (D_0) as shown in Figure 2 (c). It is given by:

$$F_d = \frac{Dmax}{Do} \tag{3}$$

Davim et al. proposed adjusted delamination factor which represents the delamination more accurately as it takes into account the actual delaminated area as opposed to the conventional delamination factor. The adjusted delamination factor (F_{da}) [36] is calculated using the following formula:

$$F_{da} = F_d + A_d \frac{(F_d^2 - F_d)}{A_{max} - A_0} \tag{4}$$

where, A_{max} and A_0 are the areas of circles obtained from the diameters D_{max} and D_0respectively as shown in Figure 2 (c). A_d is the total delamination area or damaged area, which is depicted by the black area in Figure 2 (c).

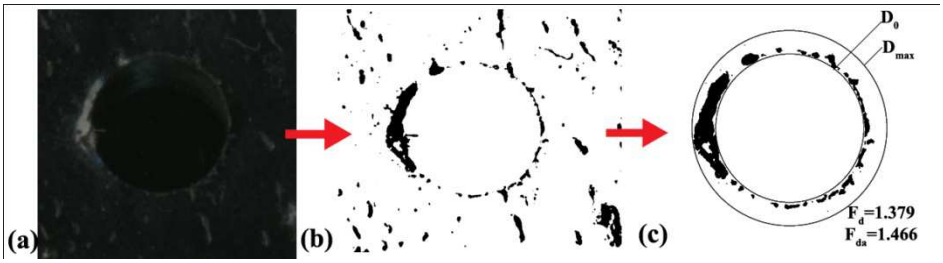

Figure 2: (a)Scanned Image of the Hole (b) Initial Processed Image (c) Final Processed Image

RESULTS AND DISCUSSION

Analysis of Tensile and Flexural Properties

The results of the mechanical tests are presented in Table 3. The stress-strain graphs of tensile test of a specimen with nanotubes and a specimen without nanotubes are shown in Figure 3. The lower slope of the graph of neat CFRP compared to COOH-MWCNTs CFRP indicates lesser Young's modulus. Tensile strength and Young's modulus were found to increase by 31.4% and 18% respectively with addition of carboxyl functionalised MWCNTs. The flexural strength increased by 43% and flexural modulus by 35.2% on adding nanotubes.

This can be attributed to the improved dispersibility in the polar epoxy resin because of better interactions with the polar carboxyl group of the nanotubes [30]. The improved interfacial interaction between the epoxy matrix and MWCNTs led to better transfer of load [31]. The characterisation of tensile failure mode was done according to ASTM D3039-17. All specimens were observed to have a failure mode of SGM (Splitting Gauge Middle) which meant it split at the middle of the gauge length. This is shown in Figure 4.

Table 3: Mechanical Properties of Specimens Tested

wt.% of COOH-MWCNTs filler	Ultimate Tensile Strength (MPa)	Young's Modulus (MPa)	Flexural Strength(MPa)	Flexural Modulus (GPa)
0	344.67 (±10.22)	7342.143 (±236.2)	423.87 (±32.8)	67.13(±3.1)
0.3	453 (±11.33)	8661.85 (±206.67)	606.3 (±69.8)	90.76(±6.32)

Correlation between $F_{da}$and Cutting Parameters

The correlation between F_{da} and drilling parameters was obtained using quadratic response surface modelling. The quadratic model of response equation in uncoded units is:

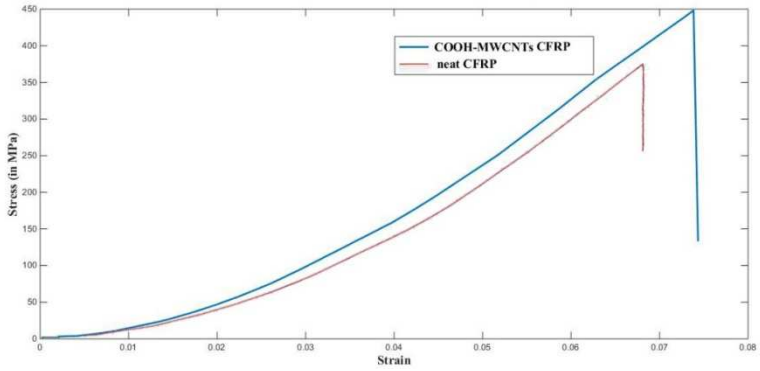

Figure 3: Stress-Strain Graph Obtained from the Tensile Test of CFRP with and without MWCNTs

Figure 4: Tensile Failure of COOH-MWCNTs CFRP

Neat CFRP

$$F_{da} = -0.717272 + 0.00223761 * N + 0.0558613 * f - 0.0102381 * \theta + 0.288256 * d - 7.49495e\text{-}07 * N^2 - 0.00127818 * f^2 + 3.84972e\text{-}05 * \theta^2 - 0.0132386 * d^2 - 1.20833e\text{-}06 * N * f + 1.77083e\text{-}06 * N * \theta - 6.46875e\text{-}05 * N * d - 7.23214e\text{-}05 * f * \theta - 0.00060625 * f * d + 0.000220982 * \theta * d \quad (5)$$

$R^2=0.979$ Adjusted $R^2=0.960$

CFRP with 0.3% MWCNTs

$$F_{da} = 0.246394 + 0.000713662 * N + 0.0155538 * f + 0.00127614 * \theta + 0.0872516 * d - 2.50337e\text{-}07 * N^2 - 0.000181212 * f^2 - 1.03587e\text{-}05 * \theta^2 - 0.00425758 * d^2 - 8.75e\text{-}07 * N * f + 7.8869e\text{-}07 * N * \theta + -1.92708e\text{-}05 * N * d - 5.26786e\text{-}05 * f * \theta - 0.00020625 * f * d + 0.000145089 * \theta * d \quad (6)$$

$R^2=0.966$ Adjusted $R^2=0.934$

where, N is the spindle speed in rpm, f is the feed rate in mm/min, θ is the point angle in degrees and d is the drill diameter in mm. Table4 shows the experimental F_{da} values, F_{da} values predicted by RSM and percentage errors.

The scatter plots presented in Figures 5 (a) and (b) show the comparison of experimental F_{da}values with the F_{da}values predicted by RSM model. A high value of R^2results in a good correlation between the experimentally obtained and predicted values, implying an excellent goodness of fit. Residual analysis is used to check the accuracy of the model[37]. Figures 6 (a) and (b) show the normal probability plots for F_{da}. The residuals are seen to closely follow the straight line, indicating a normal distribution of the errors and a good model accuracy.

Table 4: Experimental and RSM Predicted Values for F_{da}

	F_{da} **without nano tubes**			F_{da} **with nano tubes**		
Test No.	**Experimental**	**Predicted**	**Error%**	**Experimental**	**Predicted**	**Error%**
1	1.488	1.506	1.21	1.156	1.167	0.95
2	1.466	1.433	2.25	1.148	1.135	1.13
3	1.577	1.578	0.06	1.201	1.202	0.08
4	1.474	1.497	1.56	1.151	1.165	1.22
5	1.521	1.508	0.85	1.169	1.170	0.09
6	1.454	1.464	0.69	1.144	1.152	0.70
7	1.550	1.559	0.58	1.192	1.190	0.17
8	1.510	1.508	0.13	1.165	1.167	0.17
9	1.780	1.768	0.67	1.270	1.263	0.55
10	1.534	1.540	0.39	1.176	1.185	0.77
11	1.811	1.816	0.28	1.290	1.290	0.00
12	1.580	1.580	0.00	1.213	1.207	0.49
13	1.803	1.795	0.44	1.289	1.282	0.54
14	1.610	1.596	0.87	1.224	1.218	0.49
15	1.802	1.822	1.11	1.287	1.295	0.62
16	1.619	1.615	0.25	1.228	1.225	0.24
17	1.740	1.746	0.34	1.256	1.259	0.24
18	1.746	1.746	0.00	1.255	1.259	0.32
19	1.747	1.746	0.06	1.251	1.259	0.64
20	1.742	1.746	0.23	1.254	1.259	0.40
21	1.766	1.748	1.02	1.265	1.260	0.40
22	1.593	1.608	0.94	1.216	1.210	0.49
23	1.644	1.691	2.86	1.240	1.242	0.16
24	1.786	1.736	2.80	1.277	1.263	1.10
25	1.750	1.744	0.34	1.259	1.250	0.71
26	1.759	1.762	0.17	1.263	1.261	0.16
27	1.611	1.600	0.68	1.225	1.202	1.88
28	1.777	1.785	0.45	1.267	1.279	0.95
29	1.746	1.746	0.00	1.251	1.259	0.64
30	1.744	1.746	0.11	1.252	1.259	0.56
Average error			**0.71**			**0.56**

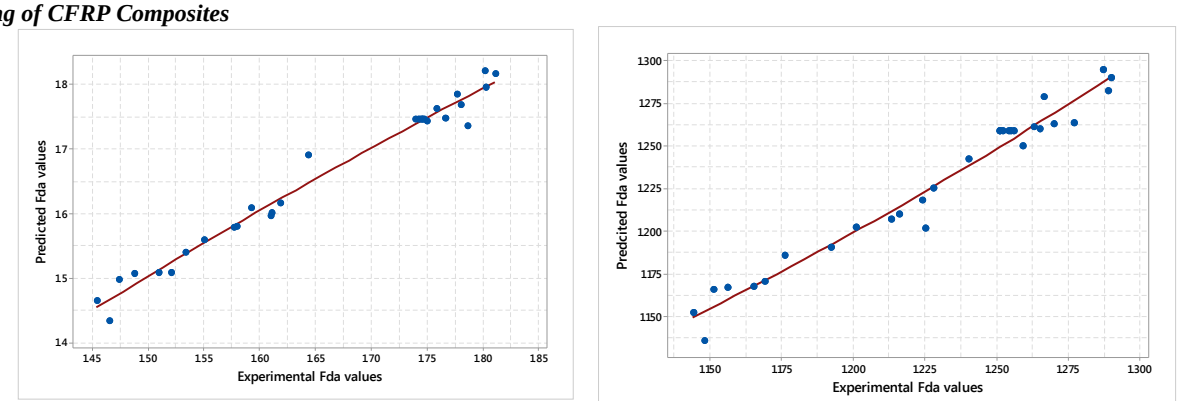

(a) (b)

Figure 5: Comparison of experimental and RSM predicted F_{da} of CFRP– (a) Without nanotubes (b) With nanotubes

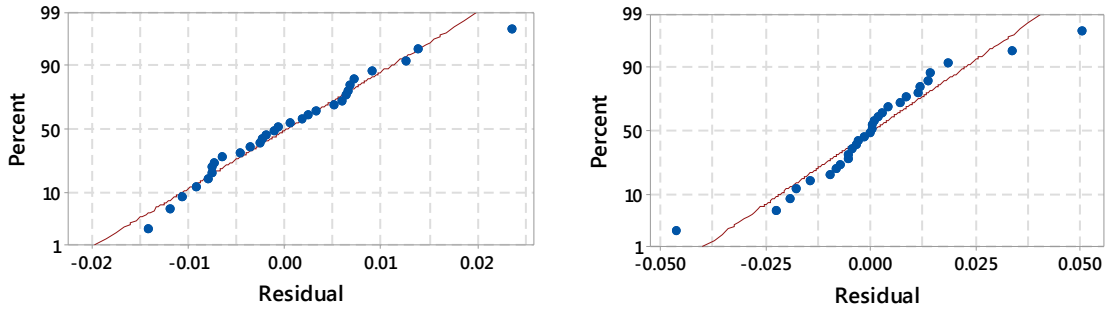

(a) (b)

Figure 6: Normal Probability Plots for $F_{da}$of CFRP – (a) without nanotubes (b) with nanotubes

Interaction Effect susing Surface Plots

3D response surface plots were generated for determining the interaction effects of drilling parameters (spindle speed, feed rate, point angle and drill diameter) on adjusted delamination factor considering two variables at a time, while the third and fourth variables are kept constant at the middle level. Figures7 (a)-(f) and 8 (a)-(f) show the interaction effect plots for neat CFRP and CFRP reinforced with MWCNTs, respectively. The interaction effects are observed to be similar for both CFRP without nanotubes and CFRP with nanotubes.

F_{da} is seen to decrease on increasing spindle speed. Higher spindle speed lead to higher cutting temperatures, and the matrix is softened thus decreasing the delamination [38]. The delamination is found to increase with an increase in feed rate due to the formation of built-up edge and local cracks at higher feed rates causing high wear of the tool and thus increased delamination [39]. The increase in point angle leads to a higher value of F_{da}. This can be attributed to an increase in thrust force at higher point angles, maximizing the delamination tendency [40]. Increasing drill diameter also increases the thrust force due to increased shear area. This leads to higher delamination [41].

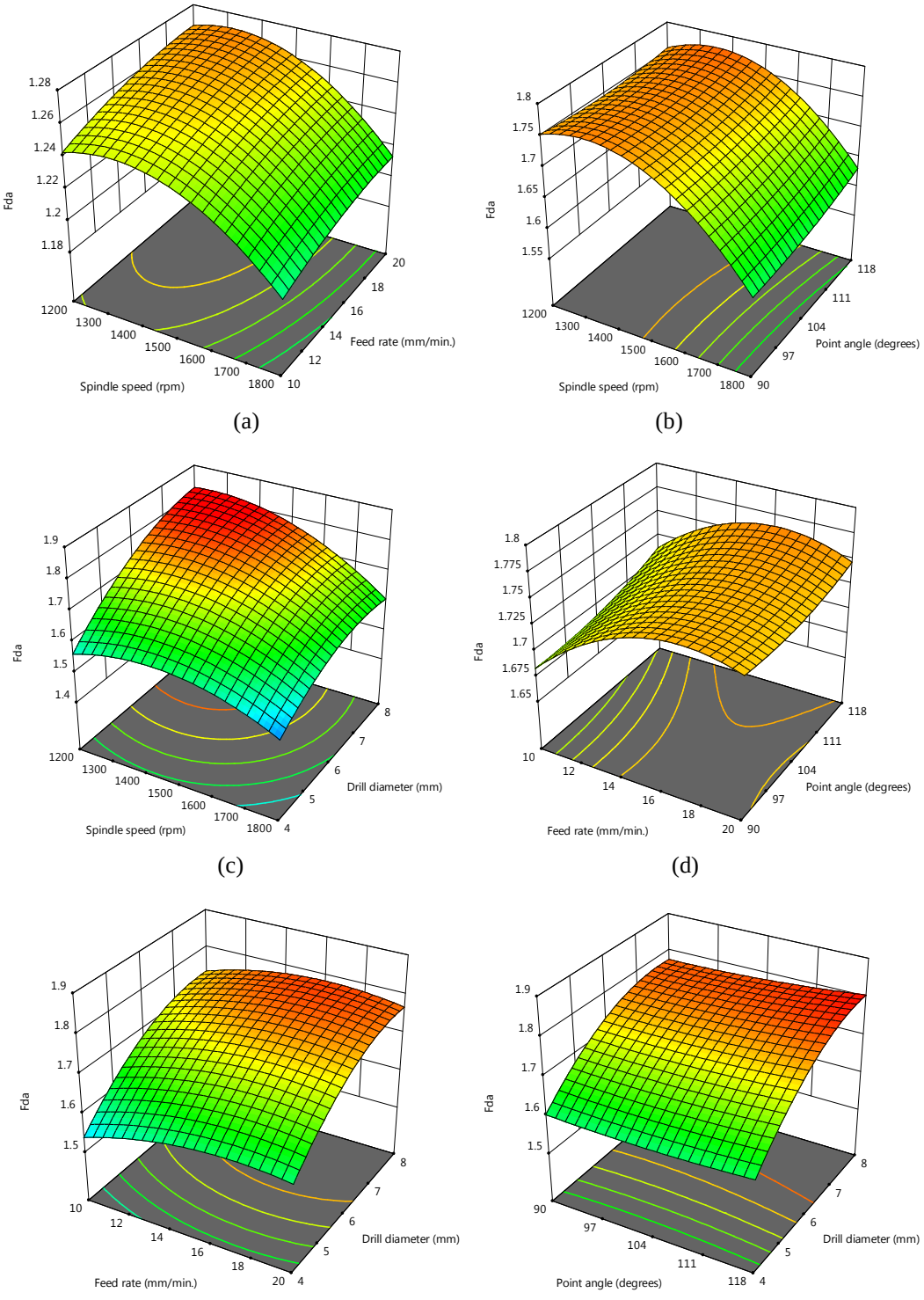

Figure 7 (a)-(f): Interaction Effect Plots for F_{da} of CFRP without Nanotubes

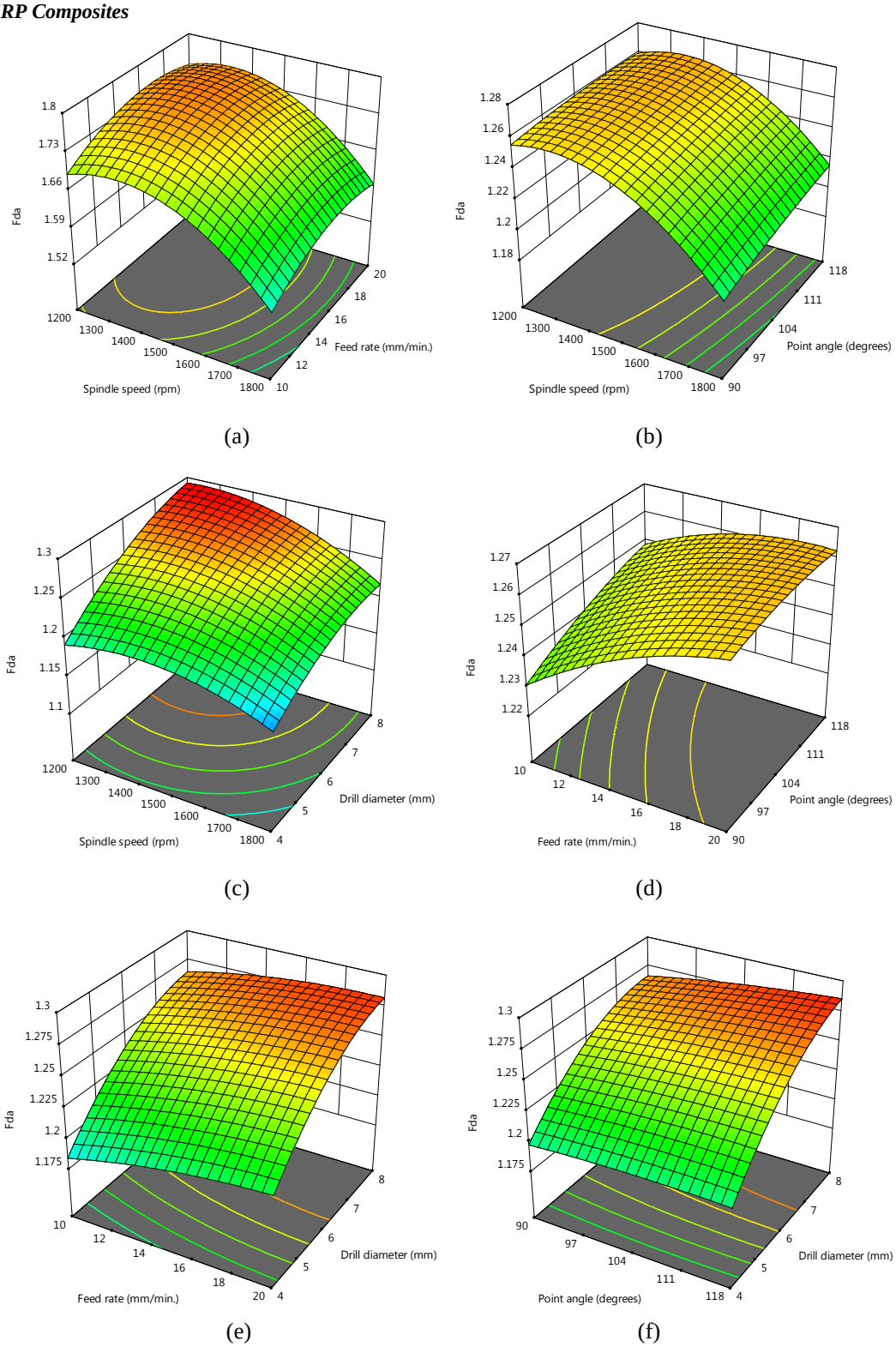

Figure 8 (a)-(f): Interaction Effect Plots for F_{da} of CFRP with Nano tubes

Optimization of Response

The experiments concerned with drilling of CFRP aim to obtain minimum delamination. The best combination of drilling parameters to achieve minimum delamination can be determined by using response surface optimization. The RSM optimized plots are displayed in Figures9 and 10. The optimum combination of parameters are

$A_3B_1C_1D_1$(Spindle speed = 1800 rpm, feed rate = 10 mm/min, point angle = 90° and drill diameter = 4 mm).

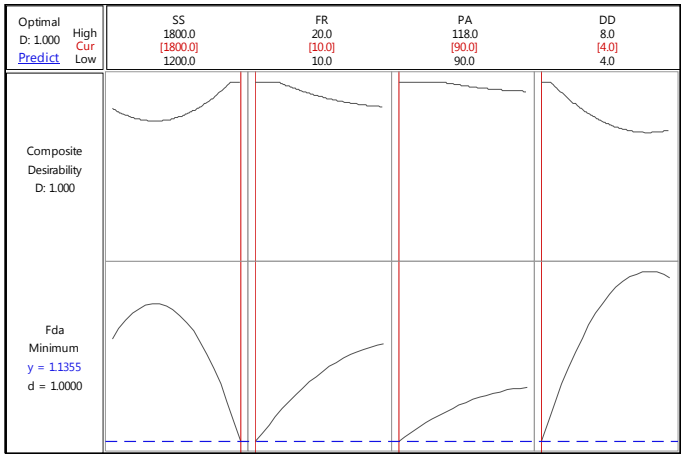

Figure 9: F_{da} Response Optimiser for Neat CFRP

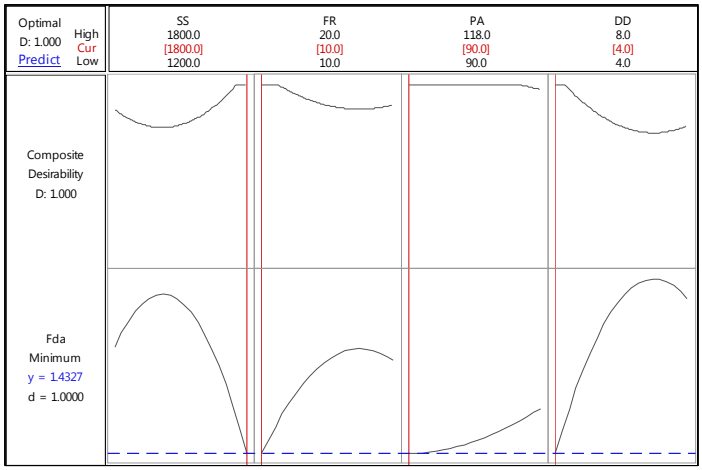

Figure 10: F_{da} Response Optimiser for CFRP with MWCNTs

Confirmation Test

The validation of optimized results obtained using RSM for the optimum parameters (Spindle speed = 1800 rpm, Feed rate= 10 mm/min, Point angle = 90 degrees, Drill diameter = 4 mm) was done by performing confirmation tests. Table 5 presents the results acquired from the confirmation tests. Small percentage errors of 2.25 for CFRP without nanotubes and 1.13 for CFRP with nanotubes indicate a close agreement of the measured F_{da} with the value predicted by RSM.

Table 5: Confirmation Test Results for F_{da}

Material	Optimum Cutting Parameters	Experimental	Prediction	Error %
CFRP	$A_3B_1C_1D_1$	1.466	1.433	2.25
CFRP with MWCNTs	$A_3B_1C_1D_1$	1.148	1.135	1.13

A_3 = 1800 rpm B_1 = 10mm/minC_1 = 90 degreesD_1 = 4mm

Validation Test

The developed RSM model's adequacy is checked by performing the validation test. To conduct the validation test, eight set of process parameters (Table 6) are chosen that have not been previously used, but lie within the experimental range. Using MINITAB 14.0 software, the adjusted delamination factor is predicted for the selected experiments using the RSM model. The experimental values, predicted values by RSM and error percentage for CFRP with neat epoxy and CFRP with epoxy reinforced with MWCNTs are given in Table 7. Low values of average error, 1.44 % for neat CFRP and 1.53 % for CFRP with 0.3% MWCNTs are obtained, signifying a reasonably accurate RSM model.

Table 6: Validation Tests Experimental Layout

Test No.	Spindle Speed, rpm	Feed rate, mm/min	Point angle, degree	Drill diameter, mm
1	1200	10	90	6
2	1200	10	104	8
3	1200	20	118	6
4	1500	10	90	6
5	1500	15	118	8
6	1500	20	104	8
7	1800	10	104	6
8	1800	15	118	4

Table 7: Experimentally Obtained and RSM Predicted Results of F_{da} for the Validation Tests

	F_{da} without nanotubes			F_{da} with nanotubes		
Test No.	Experimental	RSM predicted	Error%	Experimental	RSM predicted	Error%
1	1.653	1.691	2.25	1.246	1.233	1.04
2	1.813	1.775	2.14	1.248	1.276	2.24
3	1.749	1.744	0.29	1.283	1.261	1.71
4	1.721	1.683	2.26	1.259	1.230	2.30
5	1.799	1.807	0.44	1.276	1.285	0.71
6	1.741	1.769	1.58	1.287	1.281	0.47
7	1.58	1.555	1.61	1.231	1.195	2.92
8	1.532	1.518	0.92	1.156	1.166	0.87
Average error			**1.44**			**1.53**

Influence of MWCNTs on Delamination

Table 8 shows the summary of adjusted delamination factors. From the table, it can be seen that the addition of MWCNTs to CFRP composites led to a significantly lower value of F_{da} for all the experiments, with an average decrease in F_{da} by 25.74%. The reason for this can be attributed to an improvement in thermal conductivity of CFRP on addition of MWNCTs and an increased interlaminar bonding [42]. CFRP composites with neat epoxy tend to undergo higher damage on drilling due to maximum pull out of the matrix. This is caused by higher values of thrust force generated during drilling. On addition of nanotubes to the composite, the matrix pull out reduces due to an enhanced flexural strength. Hence, less damage occurs during drilling leading to lesser delamination [21]. Another reason for a decrease in delamination on addition of MWCNTs can be attributed to the fact that the chip formation is aided when MWCNTs are added, due to the formation of nanotube agglomerates causing less friction between the tool edge and CFRP laminates [43].

Table 8: Summary of Adjusted Delamination Factors

Test No.	F_{da} without nano tubes	F_{da} with nano tubes	% Decrease
1	1.488	1.156	22.31
2	1.466	1.148	21.69
3	1.577	1.201	23.84
4	1.474	1.151	21.91
5	1.521	1.169	23.14
6	1.454	1.144	21.32
7	1.550	1.192	23.10
8	1.510	1.165	22.85
9	1.780	1.270	28.65
10	1.534	1.176	23.34
11	1.811	1.290	28.77
12	1.580	1.213	23.23
13	1.803	1.289	28.51
14	1.610	1.224	23.98
15	1.802	1.287	28.58
16	1.619	1.228	24.15
17	1.740	1.256	27.82
18	1.746	1.255	28.12
19	1.747	1.251	28.39
20	1.742	1.254	28.01
21	1.766	1.265	28.37
22	1.593	1.216	23.67
23	1.644	1.240	24.57
24	1.786	1.277	28.50
25	1.750	1.259	28.06
26	1.759	1.263	28.20
27	1.611	1.225	23.96
28	1.777	1.267	28.70
29	1.746	1.251	28.35
30	1.744	1.252	28.21
Average decrease			**25.74**

CONCLUSIONS

Tensile and flexural tests were conducted on neat CFRP and COOH-MWCNTs modified CFRP. Drilling tests were performed on CFRP without nano tubes and CFRP with nano tubes. Digital image processing was used to determine the adjusted delamination factor of the drilled holes. The effects of drilling parameters (spindle speed, feed rate, point angle and drill diameter) on delamination were examined using response surface methodology. The influence of functionalised MWCNTs on delamination was studied. Based on the experimental results, the following conclusions were drawn:

- The addition of MWNCTs led to an improvement in tensile strength by 31.4%, Young's modulus by 18%, flexural strength by 43% and flexural modulus by 35.2% compared to neat CFRP composites.
- An equation of second order correlating the adjusted delamination factor with the drilling parameters was developed using RSM. High values of correlation coefficient (R^2), 0.979 for neat CFRP composites and 0.966 for COOH-MWCNTs CFRP nanocomposites were obtained, indicating a highly accurate model.
- The influence of drilling parameters on delamination was studied using interaction plots. Delamination was observed to decrease with an increase in spindle speed, while an increase in feed rate, point angle and drill

diameter led to an increase in delamination.

- The minimum delamination was observed at level 3 of spindle speed (1800rpm), level 1 of feed rate (10mm/min), level 1 of point angle (90°) and level 1 of drill diameter (4 mm).
- The adjusted delamination factor was on an average 25.74% less for COOH-MWCNTs modified CFRP nano composites compared to neat CFRP composites. The reasons for this were attributed to improved thermal conductivity, increased inter laminar strength and less matrix pull out in MWCNTs modified CFRP nano composites.

ACKNOWLEDGEMENTS

The authors would like to acknowledge Manipal Institute of Technology, Manipal Academy of Higher Education, Manipal for providing the facilities to conduct the research work.

REFERENCES

1. *Liu, D., Tang, Y., & Cong, W. L. (2012). A review of mechanical drilling for composite laminates. Composite Structures, 94(4), 1265-1279.*
2. *Wong, T. L., Wu, S. M., & Croy, G. M. (1982, October). An analysis of delamination in drilling composite materials. In 14th national SAMPE technical conference (Vol. 47, pp. 481-483).*
3. *Rajakumar, I. P. T., Hariharan, P., & Srikanth, I. (2013). A study on monitoring the drilling of polymeric nanocomposite laminates using acoustic emission. Journal of Composite Materials, 47(14), 1773-1784.*
4. *Kishore, R. A., Tiwari, R., Rakesh, P. K., Singh, I., & Bhatnagar, N. (2011). Investigation of drilling in fibre-reinforced plastics using response surface methodology. Proceedings of the Institution of Mechanical Engineers, Part B: Journal of Engineering Manufacture, 225(3), 453-457.*
5. *Arul, S., Vijayaraghavan, L., Malhotra, S. K., & Krishnamurthy, R. (2006). The effect of vibratory drilling on hole quality in polymeric composites. International Journal of Machine Tools and Manufacture, 46(3-4), 252-259.*
6. *Zitoune, R., & Collombet, F. (2007). Numerical prediction of the thrust force responsible of delamination during the drilling of the long-fibre composite structures. Composites Part A: Applied Science and Manufacturing, 38(3), 858-866.*
7. *Seif, M. A., Khashaba, U. A., & Rojas-Oviedo, R. (2007). Measuring delamination in carbon/epoxy composites using a shadow moiré laser based imaging technique. Composite structures, 79(1), 113-118.*
8. *Stone, R., & Krishnamurthy, K. (1996). A neural network thrust force controller to minimize delamination during drilling of graphite-epoxy laminates. International Journal of Machine Tools and Manufacture, 36(9), 985-1003.*
9. *Durão, L. M. P., Gonçalves, D. J., Tavares, J. M. R., de Albuquerque, V. H. C., Vieira, A. A., & Marques, A. T. (2010). Drilling tool geometry evaluation for reinforced composite laminates. Composite structures, 92(7), 1545-1550.*
10. *Shyha, I., Soo, S. L., Aspinwall, D., & Bradley, S. (2010). Effect of laminate configuration and feed rate on cutting performance when drilling holes in carbon fibre reinforced plastic composites. Journal of materials processing technology, 210(8), 1023-1034.*
11. *Capello, E. (2004). Workpiece damping and its effect on delamination damage in drilling thin composite laminates. Journal of Materials Processing Technology, 148(2), 186-195.*

12. Tsao, C. C., & Hocheng, H. (2005). Effects of exit back-up on delamination in drilling composite materials using a saw drill and a core drill. International Journal of Machine Tools and Manufacture, 45(11), 1261-1270.

13. Murphy, C., Byrne, G., & Gilchrist, M. D. (2002). The performance of coated tungsten carbide drills when machining carbon fibre-reinforced epoxy composite materials. Proceedings of the Institution of Mechanical Engineers, Part B: Journal of Engineering Manufacture, 216(2), 143-152.

14. Hocheng, H., & Tsao, C. C. (2005). The path towards delamination-free drilling of composite materials. Journal of materials processing technology, 167(2-3), 251-264.

15. Khashaba, U. A., El-Sonbaty, I. A., Selmy, A. I., & Megahed, A. A. (2010). Machinability analysis in drilling woven GFR/epoxy composites: Part I–Effect of machining parameters. Composites Part A: Applied Science and Manufacturing, 41(3), 391-400.

16. Heisel, U., & Pfeifroth, T. (2012). Influence of point angle on drill hole quality and machining forces when drilling CFRP. Procedia CIRP, 1, 471-476.

17. Abrao, A. M., Rubio, J. C., Faria, P. E., & Davim, J. P. (2008). The effect of cutting tool geometry on thrust force and delamination when drilling glass fibre reinforced plastic composite. Materials & Design, 29(2), 508-513.

18. Kim, D., & Ramulu, M. (2004). Drilling process optimization for graphite/bismaleimide–titanium alloy stacks. Composite structures, 63(1), 101-114.

19. Feito, N., Díaz-Álvarez, J., López-Puente, J., & Miguelez, M. H. (2018). Experimental and numerical analysis of step drill bit performance when drilling woven CFRPs. Composite Structures, 184, 1147-1155.

20. Karimi, Z. N., Heidary, H., Yousefi, J., Sadeghi, S., & Minak, G. (2018). Experimental investigation on delamination in nanocomposite drilling. FME Transactions, 46(1), 62-69.

21. Kumar, D., & Singh, K. K. (2017). Investigation of delamination and surface quality of machined holes in drilling of multiwalled carbon nanotube doped epoxy/carbon fiber reinforced polymer nanocomposite. Proceedings of the Institution of Mechanical Engineers, Part L: Journal of Materials: Design and Applications, 1464420717692369.

22. Rubio, J. C., Abrao, A. M., Faria, P. E., Correia, A. E., & Davim, J. P. (2008). Effects of high speed in the drilling of glass fibre reinforced plastic: evaluation of the delamination factor. International Journal of Machine Tools and Manufacture, 48(6), 715-720.

23. Xie, X. L., Mai, Y. W., & Zhou, X. P. (2005). Dispersion and alignment of carbon nanotubes in polymer matrix: a review. Materials Science and Engineering: R: Reports, 49(4), 89-112.

24. Grossiord, N., Loos, J., Regev, O., & Koning, C. E. (2006). Toolbox for dispersing carbon nanotubes into polymers to get conductive nanocomposites. Chemistry of materials, 18(5), 1089-1099.

25. Sun, L., Warren, G. L., O'reilly, J. Y., Everett, W. N., Lee, S. M., Davis, D., & Sue, H. J. (2008). Mechanical properties of surface-functionalized SWCNT/epoxy composites. Carbon, 46(2), 320-328.

26. Li, N., Li, Y., Zhou, J., He, Y., & Hao, X. (2015). Drilling delamination and thermal damage of carbon nanotube/carbon fiber reinforced epoxy composites processed by microwave curing. International Journal of Machine Tools and Manufacture, 97, 11-17.

27. Gojny, F. H., Wichmann, M. H., Fiedler, B., & Schulte, K. (2005). Influence of different carbon nanotubes on the mechanical properties of epoxy matrix composites–a comparative study. Composites Science and Technology, 65(15-16), 2300-2313.

28. *Gojny, F. H., Nastalczyk, J., Roslaniec, Z., & Schulte, K. (2003). Surface modified multi-walled carbon nanotubes in CNT/epoxy-composites. Chemical physics letters, 370(5-6), 820-824.*

29. *Abdelal, N. R., Al-Saleh, M. H., & Irshidat, M. R. (2018). Utilizing vacuum bagging process to prepare carbon fiber/CNT-modified-epoxy composites with improved mechanical properties. Polymer-Plastics Technology and Engineering, 57(3), 175-184.*

30. *Gojny, F. H., Wichmann, M. H. G., Köpke, U., Fiedler, B., & Schulte, K. (2004). Carbon nanotube-reinforced epoxy-composites: enhanced stiffness and fracture toughness at low nanotube content. Composites science and technology, 64(15), 2363-2371.*

31. *Jahan, N., Narteh, A. T., Hosur, M., Rahman, M., & Jeelani, S. (2013). Effect of carboxyl functionalized MWCNTs on the cure behavior of epoxy resin. Open J Compos Mater, 3, 40-47.*

32. *Islam, M. E., Mahdi, T. H., Hosur, M. V., & Jeelani, S. (2015). Characterization of carbon fiber reinforced epoxy composites modified with nanoclay and carbon nanotubes. Procedia Engineering, 105, 821-828.*

33. *Zhou, Y., Pervin, F., Lewis, L., & Jeelani, S. (2008). Fabrication and characterization of carbon/epoxy composites mixed with multi-walled carbon nanotubes. Materials Science and Engineering: A, 475(1-2), 157-165.*

34. *Cochran, W. G.,& Cox. GM (1957) Experimental Designs. J. Willey and Sons.*

35. *Chen, W. C. (1997). Some experimental investigations in the drilling of carbon fiber-reinforced plastic (CFRP) composite laminates. International Journal of Machine Tools and Manufacture, 37(8), 1097-1108.*

36. *Davim, J. P., Rubio, J. C., & Abrao, A. M. (2007). A novel approach based on digital image analysis to evaluate the delamination factor after drilling composite laminates. Composites Science and Technology, 67(9), 1939-1945.*

37. *Montgomery, D. C. (2001). Design and analysis of experiments. John wiley & sons.*

38. *Karnik, S. R., Gaitonde, V. N., Rubio, J. C., Correia, A. E., Abrão, A. M., & Davim, J. P. (2008). Delamination analysis in high speed drilling of carbon fiber reinforced plastics (CFRP) using artificial neural network model. Materials & Design, 29(9), 1768-1776.*

39. *Uhlmann, E., Richarz, S., Sammler, F., & Hufschmied, R. (2016). High Speed Cutting of carbon fibre reinforced plastics. Procedia Manufacturing, 6, 113-123.*

40. *Gaitonde, V. N., Karnik, S. R., Rubio, J. C., Correia, A. E., Abrao, A. M., & Davim, J. P. (2011). A study aimed at minimizing delamination during drilling of CFRP composites. Journal of composite materials, 45(22), 2359-2368.*

41. *Abrao, A. M., Faria, P. E., Rubio, J. C., Reis, P., & Davim, J. P. (2007). Drilling of fiber reinforced plastics: A review. Journal of Materials Processing Technology, 186(1-3), 1-7.*

42. *Samuel, J., Dikshit, A., DeVor, R. E., Kapoor, S. G., & Hsia, K. J. (2009). Effect of carbon nanotube (CNT) loading on the thermomechanical properties and the machinability of CNT-reinforced polymer composites. Journal of Manufacturing Science and Engineering, 131(3), 031008.*

43. *Arora, I., Samuel, J., & Koratkar, N. (2013). Experimental investigation of the machinability of epoxy reinforced with graphene platelets. Journal of Manufacturing Science and Engineering, 135(4), 041007.*